Property change of unstable fixed point and phase synchronization in controlling spatiotemporal chaos by a periodic signal

Haibo Sang and Kaifen He
The Key Laboratory of Beam and Materials Modification of Education Ministry, Beijing Normal University, 100875, Beijing, China; Institute of Low Energy Nuclear Physics, Beijing Normal University, 100875, Beijing, China; and Beijing Radiation Centre, 100875, Beijing, China
(Received 15 February 2007; published 4 September 2007)

Mechanisms for the suppression of spatiotemporal chaos (STC) in one-dimensional driven drift-wave system to a spatially regular state by a periodic signal are investigated. In the driving wave coordinate, by transforming the system to a set of coupled oscillators (modes) moving in a periodic potential, it is found that the modes can be enslaved one by one through phase synchronization (PS) by the control signal; for some modes frequency-locking occurs while the other modes display multilooping PS without frequency-locking. Further study of the linear behavior of the modes shows that the saddle point embedded in the STC is changed to an unstable focus, which makes it possible for the imperfect PS to change to a perfect functional one, leading to the suppression of the STC.

DOI: 10.1103/PhysRevE.76.036202 PACS number(s): 05.45.Gg, 05.45.Jn

I. INTRODUCTION

Controlling and synchronizing chaos are of great importance in nature and in technical applications. The growing interest in this field stems from the pioneering works done by Ott, Grebogi, and Yorke in 1990 [1] in chaos control, and by Carroll and Pecora in chaos synchronization [2]. Since then some techniques for controlling temporal chaos have been developed that can be divided into two categories: feedback [3] and nonfeedback method [4]. Recently researchers have extended these techniques to control spatiotemporal chaos (STC) [5], which deserves to be addressed because of its wide applications in plasma, laser devices, and various chemical and biological systems.

In recent years, it has been understood that coupling can synchronize not only periodic, but also chaotic systems. Depending on the type and strength of the coupling, several types of chaotic synchronization can be distinguished. The strongest one is the complete synchronization when the states of coupled systems converge, irrespective of the mismatch in initial conditions [6]. In a wider context, the state of the driven system is a function of that of the driving one, which is called generalized synchronization [7]. Among the forms of chaotic synchronization, phase synchronization (PS) is a relatively weak one. It describes the identity in the phases of nonidentical chaotic oscillators, whereas their amplitudes may remain chaotic and uncorrelated [8]. It has been shown to play a crucial role in a wide range of situations including laser, plasma, fluid and many physiological systems such as brain function, kidney function, human heartbeat and respiration [9]. It is worth mentioning that when external periodic force is applied to a chaotic chemical oscillator in the experiments on the electrodissolution of Ni in sulfuric acid solution, PS occurs with increasing the amplitude of the force [10]. Moreover, PS between oscillators can be perfect or imperfect; e.g., it is found that when the intrinsic time scale is not bounded from above due to an embedded saddle point, coupled oscillators in the Lorenz system can adjust themselves to imperfect synchronization [11].

However, the mechanism of controlling chaos and its relation with synchronization are lack of investigation for space-time dependent systems. Among them, the one-dimensional drift-wave equation driven by a sinusoidal wave in plasmas and fluids is a typical nonlinear equation to show STC. In a previous work [12], an STC state is suppressed successfully in the driven one-dimensional drift-wave system by adding an external periodic signal with proper frequency and strength. Moreover, by transforming the nonlinear wave system to a set of coupled oscillators moving in the potential of the steady wave, the controlling mechanism is regarded simply as the slaving principle. In this paper, PS between the oscillators is found in controlling the STC first. Here PS of two coupled oscillators m, n is defined as $\Delta\alpha_{m,n} \equiv |\alpha_m(t) - \alpha_n(t)| < \text{const}$, and α_m, α_n are their phases, respectively [8]. We will show that two types of responses of the internal modes to the external periodic signal are observed. For some modes, the stabilization is through frequency-locking; while for the other modes, a special kind of PS without frequency-locking, namely multilooping PS is developed. Furthermore, it is found that after the control signal is added the original saddle point embedded in the STC is changed to an unstable focus. Such property change of the unstable fixed point allows the oscillators with different time scales adjusting to perfect functional phase synchronization, in contrast to the imperfect one before the control. These are the ways in which the internal modes are enslaved by the applied signal and the STC is suppressed.

II. MODEL

The nonlinear driven-drift wave equation is used as our model

$$\frac{\partial\phi}{\partial t} + a\frac{\partial^3\phi}{\partial t\partial x^2} + c\frac{\partial\phi}{\partial x} + f\phi\frac{\partial\phi}{\partial x} = -\gamma\phi - \varepsilon\sin(x-\Omega t). \quad (1)$$

If the right-hand side is zero, the equation is the regularized long-wave equation or the nonlinear drift wave equation in

Plasmas [13]. Here the 2π boundary condition, $\phi(x+2\pi,t)=\phi(x,t)$, is applied. $a<0$, c, f, and γ are fixed parameters. For Ω in certain regimes, e.g., $\Omega=0.65$, $\varepsilon=0.22$ as in the present work, a crisis occurs at a critical $\varepsilon=\varepsilon_c$ which induces transition from spatially regular state to STC [14].

To control the STC, we add a small temporally periodic signal $\eta\cos(\omega t)$ to the right-hand side of Eq. (1). If frequency ω and strength η are properly chosen, the STC can be controlled successfully to a spatially regular state. In the following, we use $\omega=0.756$, $\eta=0.1$ for the periodic signal.

To study the behaviors of different scales it is helpful to shift the system to a driver frame with $z=x-\Omega t$, $\tau=t$, in which the steady wave $\phi_0(z)$ satisfies $\partial\phi_0(z)/\partial\tau=0$. By setting $\phi(z,\tau)=\phi_0(z)+\delta\phi(z,\tau)$, the perturbation wave $\delta\phi(z,\tau)$ is governed by

$$\frac{\partial}{\partial\tau}\left(1+a\frac{\partial^2}{\partial z^2}\right)\delta\phi=\Omega\frac{\partial}{\partial z}\left(1+a\frac{\partial^2}{\partial z^2}\right)\delta\phi-c\frac{\partial\delta\phi}{\partial z}-f\phi_0\frac{\partial\delta\phi}{\partial z}-f\delta\phi\frac{\partial\phi_0}{\partial z}-f\delta\phi\frac{\partial\delta\phi}{\partial z}-\gamma\delta\phi+\eta\cos(\omega\tau). \tag{2}$$

Let us expand $\phi_0(z)$ and $\delta\phi(z,\tau)$ into Fourier modes, respectively,

$$\phi_0(z)=A_0+\lim_{N\to\infty}\sum_{k=1}^{N}A_k\cos(kz+\theta_k),$$

$$\delta\phi(z,\tau)=b_0(\tau)+\lim_{N\to\infty}\sum_{k=1}^{N}b_k(\tau)\cos[kz+\alpha_k(\tau)].$$

Here mode $k=0$ is included because the control signal $\eta\cos(\omega\tau)$ is added on $k=0$. For given parameters, $\{A_k,\theta_k\}$ can be solved from the equation of the steady wave $\phi_0(z)$. It is easy to see that $\{A_k,\theta_k\}$, or equivalently $\phi_0(z)$, is a fixed point in the Fourier space [15]. Substituting the solution of $\{A_k,\theta_k\}$, we get a set of equations for $\{b_k(\tau),\alpha_k(\tau)\}$,

$$\frac{db_0}{d\tau}=-\gamma b_0+\eta\cos(\omega\tau),$$

$$\frac{db_k}{d\tau}=N_k(\tau)+\frac{fkb_0A_k\sin(\theta_k-\alpha_k)}{1-ak^2},$$

$$\frac{d\alpha_k}{d\tau}=M_k(\tau)-\frac{fk(A_0+b_0)}{1-ak^2}-\frac{fkb_0A_k\sin(\theta_k-\alpha_k)}{(1-ak^2)b_k}, \tag{3}$$

where

$$N_k(\tau)=-\frac{\gamma b_k}{1-ak^2}+\frac{fk}{2(1-ak^2)}\Bigg\{\sum_{l+l'=k}\left[A_lb_{l'}\sin(\theta_l+\alpha_{l'}-\alpha_k)+\frac{1}{2}b_lb_{l'}\sin(\alpha_l+\alpha_{l'}-\alpha_k)\right]+\sum_{l-l'=k}\left[A_lb_{l'}\sin(\theta_l-\alpha_{l'}-\alpha_k)+\frac{1}{2}b_lb_{l'}\sin(\alpha_l-\alpha_{l'}-\alpha_k)\right]+\sum_{l'-l=k}\left[A_lb_{l'}\sin(-\theta_l+\alpha_{l'}-\alpha_k)+\frac{1}{2}b_lb_{l'}\times\sin(-\alpha_l+\alpha_{l'}-\alpha_k)\right]\Bigg\},$$

$$M_k(\tau)=-k\left(\frac{c}{1-ak^2}-\Omega\right)-\frac{fk}{2(1-ak^2)b_k}\times\Bigg\{\sum_{l+l'=k}\left[A_lb_{l'}\cos(\theta_l+\alpha_{l'}-\alpha_k)+\frac{1}{2}b_lb_{l'}\cos(\alpha_l+\alpha_{l'}-\alpha_k)\right]+\sum_{l-l'=k}\left[A_lb_{l'}\cos(\theta_l-\alpha_{l'}-\alpha_k)+\frac{1}{2}b_lb_{l'}\cos(\alpha_l-\alpha_{l'}-\alpha_k)\right]+\sum_{l'-l=k}\left[A_lb_{l'}\cos(-\theta_l+\alpha_{l'}-\alpha_k)+\frac{1}{2}b_lb_{l'}\cos(-\alpha_l+\alpha_{l'}-\alpha_k)\right]\Bigg\}$$

$$(k=1,2,\ldots,N\to\infty).$$

$\{b_k(\tau),\alpha_k(\tau)\}$ are thus obtained and can be regarded as a set of coupled oscillators whose motions are influenced by the steady wave $\phi_0(z)$ as if the latter is a potential [see also Eq. (2)].

The energy of system (1) is defined by the integral $E(t)=(1/2\pi)\int_0^{2\pi}(1/2)[\phi^2(x,t)-a(\partial\phi/\partial x)^2]dx$ and, accordingly, the energy perturbation is $\delta E(\tau)\equiv E(\tau)-E_0=\Sigma_k\delta E_k$, where $E_0=E(\phi_0)$ is a constant and $\delta E_k=(1-ak^2)[A_kb_k\cos(\theta_k-\alpha_k)/2+b_k^2/4]$ is the mode energy of the perturbation wave $\delta\phi(z,\tau)$.

III. TWO TYPES OF PS AFTER CONTROL

In the previous work [16], it has been shown that before control in the STC state the mode phases $\{\alpha_k\}$ evolute with

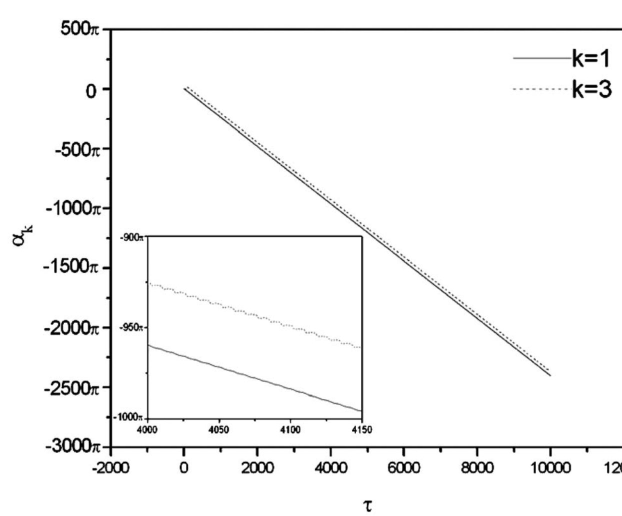

FIG. 1. Temporal evolution of phases $k=1$ and 3 with control signal.

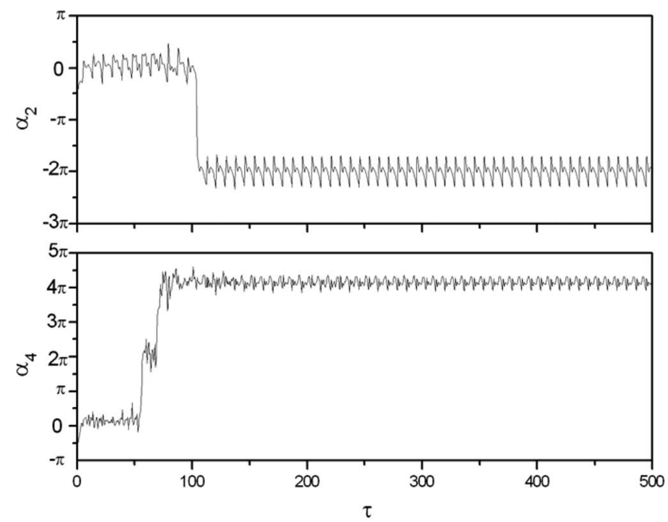

FIG. 2. Temporal evolution of phases $k=2$ and 4 with control signal.

time disorderly, and an on-off collective imperfect PS can be developed among different spatial scales. After the proper periodic signal is added, the turbulent state is suppressed to a regular laminar state, where the motion of the mode phases $\{\alpha_k\}$ look very regular. Two types of PS, that is, PS with and without frequency-locking, are found according to different responses of the internal modes to the control signal. For example, on average, the phases of modes $k=1,3$ shown in Fig. 1 are synchronized with the external periodic signal in terms of frequency-locking. The averaged frequencies (tangencies of the curves in Fig. 1) are equal to that of the external signal respectively, that is, frequency-locking takes place with the ratio $\bar{\omega}_1:\bar{\omega}_3:\omega=1:1:1$. For the other modes, the phases transit gradually from chaotic to quasiperiodic oscillations and in the asymptotic state the averaged frequencies are all zero, for example $\bar{\omega}_{k=2,4}=0$ as given in Fig. 2. It seems that these phases are doing nothing more than adjusting with each other to achieve synchronization. Intermittent phase slips occur frequently before PS is achieved. It is likely that more phase slips appear when the wave number k is increased. The phases differences between $k=1,3$ and $k=2,4$ are shown in Fig. 3, from which one can confirm that PS has been arrived for these modes respectively in the asymptotic state.

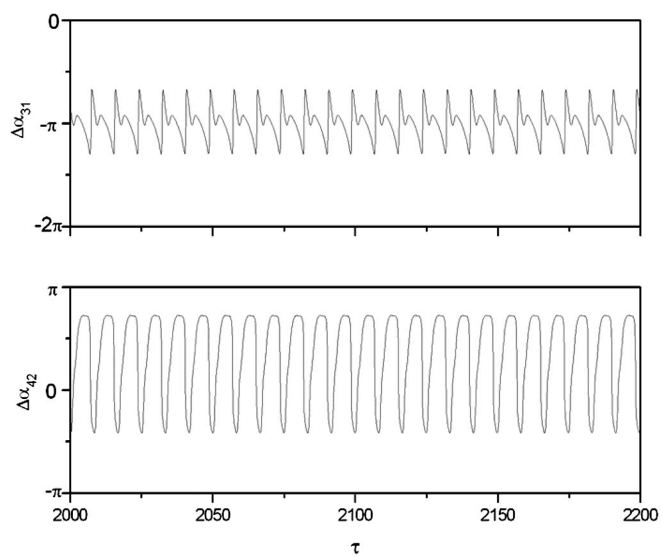

FIG. 3. Temporal evolution of phase differences between $k=1,3$ and $k=2,4$ in the asymptotic state with control signal.

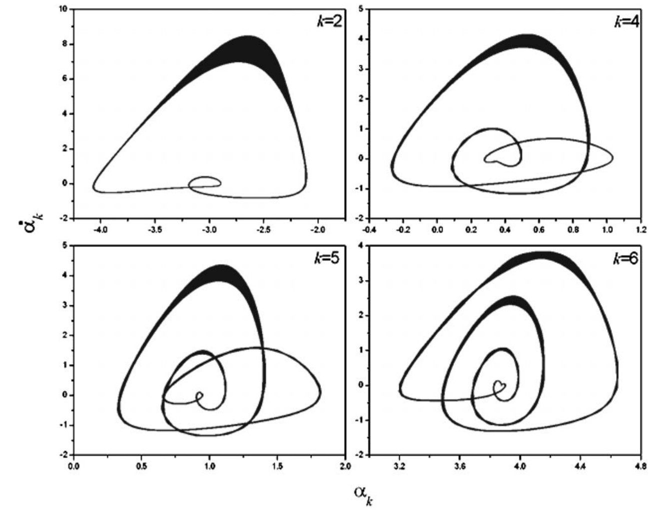

FIG. 4. Phase plots $\alpha_k \sim \dot{\alpha}_k$ of $k=2$, 4, 5, and 6 with control signal.

The phase plot $\alpha_k - \dot{\alpha}_k$ is very helpful for clarifying their motions in the controlled spatially regular state. For modes $k=1,3$ i.e., those modes with frequency-locking, there is only one loop in the phase plot. However, it is very interesting that for the modes without frequency-locking the phase plots show multilooping curves as shown in Fig. 4, we therefore name this type of PS as multilooping PS. It is a kind of generalized synchronization (GS), i.e., a functional relation exists between the states of the responder and driver [17].

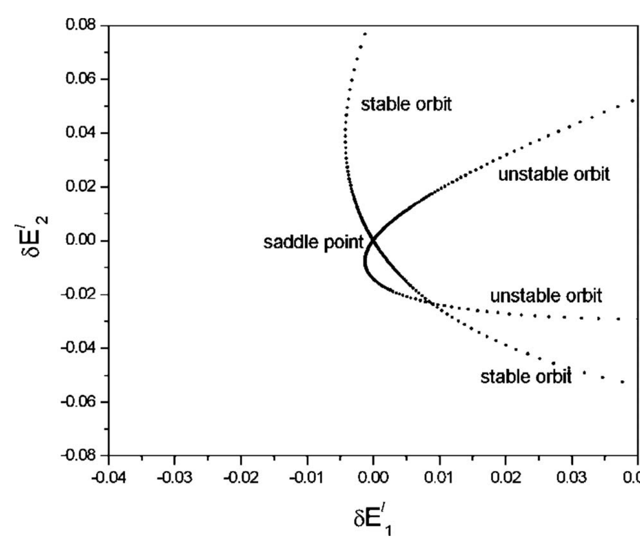

FIG. 5. Stable and unstable orbits of embedded saddle point in $\delta E_1^l - \delta E_2^l$ space without control signal.

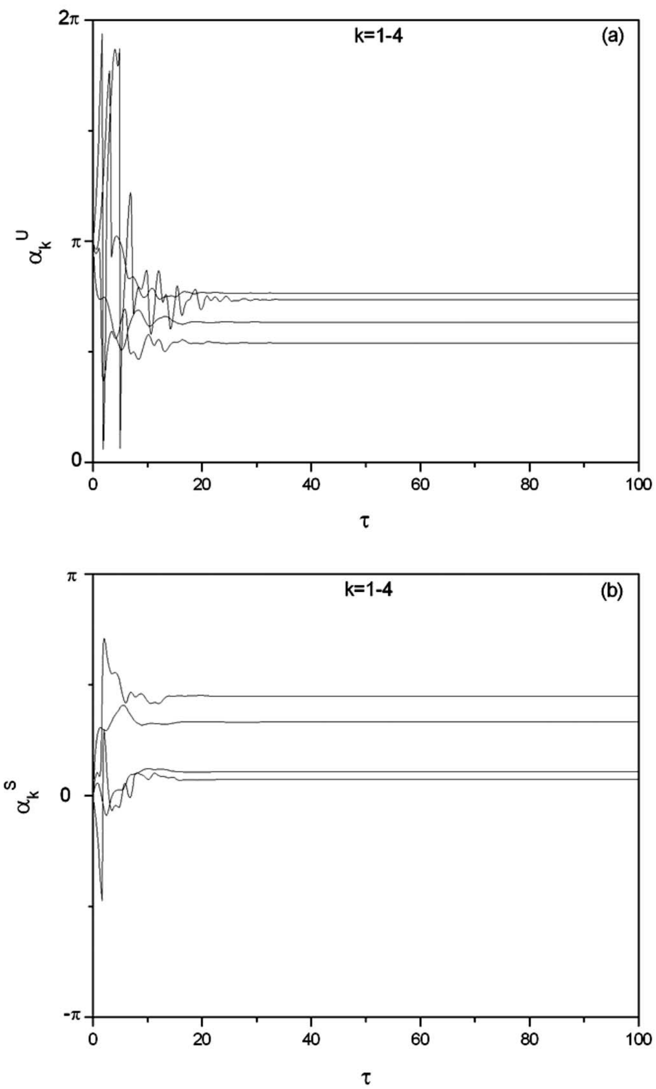

FIG. 6. Linear evolution of α_k without control signal.

Moreover, it is also found from Fig. 4 that the looping number increases with the wave number k. In this context, it would be helpful to study the linear dispersion relation of undriven drift-wave ($\varepsilon=\gamma=f=0$) obtained from Eq. (2), where the natural frequency $\omega_k^l=|kc/(1-ak^2)-k\Omega|$ increases with the wave number k. This fact is in accordance with the phenomenon that the looping number increases with the wave number k. But under the action of the dissipation, drift, nonlinearity and the external periodic signal, the mode frequencies $\{\omega_k\}$ are adjusted from $\{\omega_k^l\}$, no simple relation is found between the looping number and the wave number k.

IV. PROPERTY CHANGE OF THE UNSTABLE FIXED POINT IN CONTROLLING THE STC

By omitting the nonlinear term $b_l b_{l'}$ in Eq. (3), the evolution of linear modes $\{b_k^l(\tau),\alpha_k^l(\tau)\}$ can be studied, from which the mechanism of controlling STC can be further clarified. Here and in the following the superscript l indicates the linear approximation.

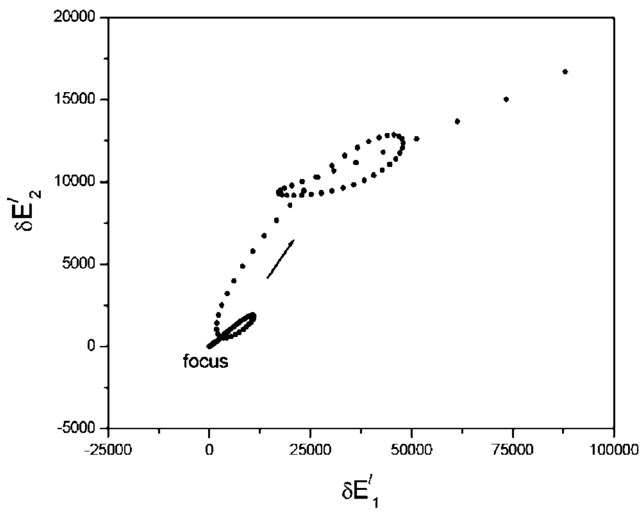

FIG. 7. Orbit of fixed point in $\delta E_1^l-\delta E_2^l$ space with control signal.

In Ref. [15], it has been shown that before the control, the fixed point $\phi_0(z)$ is a saddle one embedded in the STC. For the convenience of comparison, here we present Fig. 5 showing the evolution of δE_1^l and δE_2^l with time τ in $\delta E_1^l-\delta E_2^l$ space; here the superscript l indicates that δE^l is calculated from $\{b_k^l(\tau),\alpha_k^l(\tau)\}$. They are the two unstable-stable orbits (UO-SO) of the saddle point, respectively. Due to the saddle-node instability, the initially small amplitudes $\{b_k^l(0)\}$ of the perturbation wave increase exponentially, at the same time their phases $\{\alpha_k^l(\tau)\}$ approach constants $\{\alpha_k^U\}$ and $\{\alpha_k^S\}$ respectively as shown in Fig. 6 for $k=1-4$, where one can find the variations of $\{\alpha_k^l(\tau)\}$ along (a) the two UO and (b) the two SO. Obviously, the eigenfrequencies of the modes are all zero. It is due to the embedded saddle point that the intrinsic time scale is not bounded from above, and the synchronization of coupled oscillators $\{b_k(\tau),\alpha_k(\tau)\}$ in STC become imperfect.

However, the two UO-SO shown in Fig. 5 disappear after the proper control signal is added. There is only one orbit convoluting from the fixed point (0,0) in plot $\delta E_1^l-\delta E_2^l$, as shown in Fig. 7. Let us turn to Eq. (3) without the nonlinear terms to study the evolution of mode phases $\{\alpha_k^l(\tau)\}$. Obviously, the evolution of $k=0$ mode is independent of $k\neq 0$ mode and b_0 oscillates periodically with frequency ω. On the other hand, the equations of $\{b_k^l(\tau),\alpha_k^l(\tau)\}$ $(k\neq 0)$ all depend on b_0 and are affected by the evolution of b_0. It is found that all linear mode phases $\alpha_k^l(\tau)$ oscillate with time, as shown in Fig. 8 for $k=1-4$ as an example. Moreover, they are all frequency-locking to the external control signal with the ratio $|\bar{\omega}_k^l|:\omega=1:2$, where ω_k^l is the linear frequency of mode k. Such nonzero eigenfrequency indicates the finite intrinsic time scales, in contrast to the infinite time scale without the control. Thus we conclude that the original saddle point embedded in the STC has changed to an unstable focus.

V. DISCUSSION AND CONCLUSION

To understand further the phenomena described above, let us refer to Ref. [11], where the mechanism of perfect and

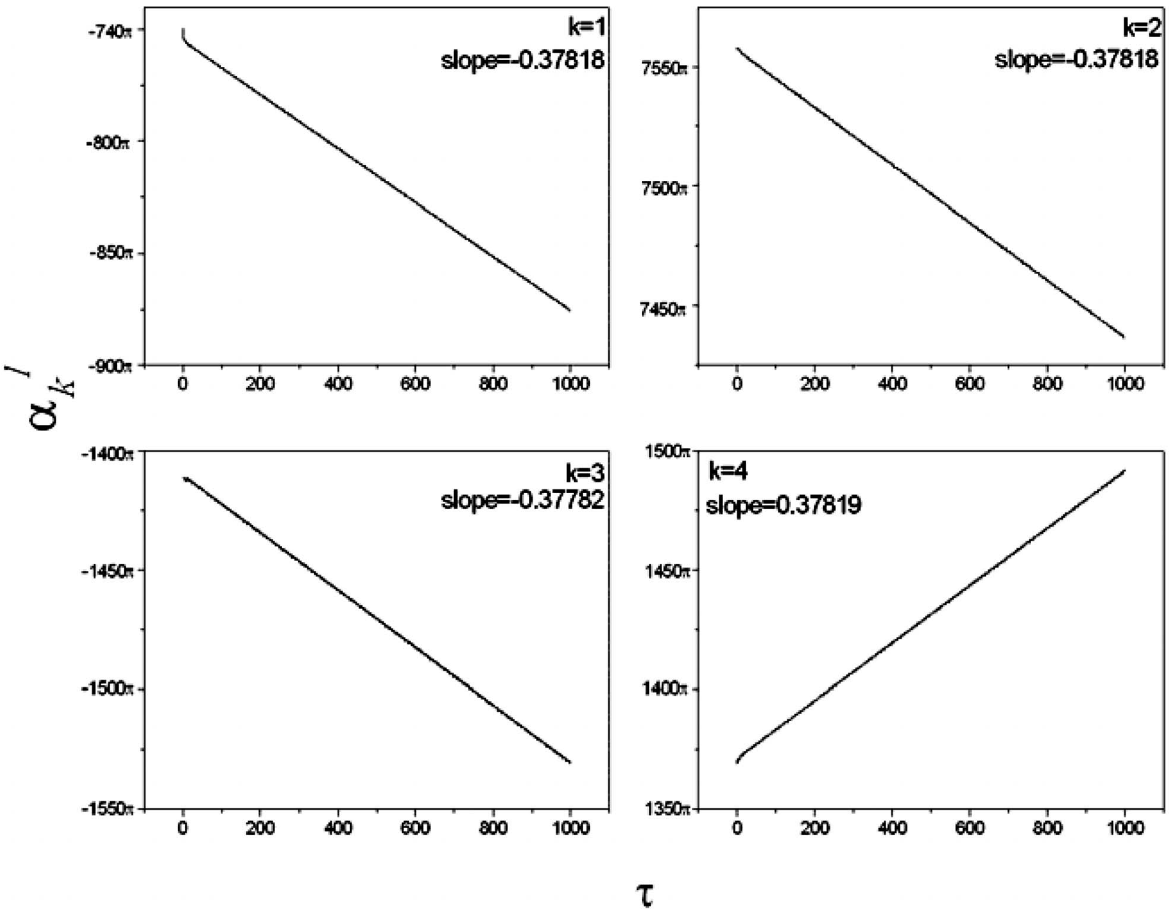

FIG. 8. Linear evolution of α_k with control signal.

imperfect PS in periodically driven Lorenz equation is studied in terms of unstable periodic orbits. It is pointed out that in the presence of weak forcing, each periodic orbit can be viewed as an individual periodically forced oscillator. If the main Arnold tongues of different periodic orbits of the autonomous system overlap, a domain common to all tongues will exist. Inside this domain, all periodic motions are locked to the same ratio by the external force, allowing the occurrence of the perfect PS. Just outside the overlap domain, synchronized motions are interrupted by phase slips, thereby the imperfect PS occurs. As to our model, the unstable periodic orbits in the STC before control can be regarded as individual periodical oscillators. When the saddle point is embedded in STC, these orbits experience the return times varying in a large range along the Poincare surface. In particular, if a chaotic orbit goes arbitrarily close to the local stable manifold of the saddle point, its return time along the Poincare surface can be arbitrarily high. The domain common to all tongues may disappear. If two mode phases tend to deviate from each other, they will be adjusted by phase slips, thus the imperfect PS occurs. Whereas after the periodic control signal is added, the saddle point is changed to an unstable focus. Since the frequencies of the orbits are locked by the external force, the return times of the orbits vary little, which enable the existence of the domain common to all the tongues. Accordingly, the modes phases can achieve the generalized perfect PS.

In summary, it is found that the original saddle point embedded in the spatiotemporal chaos is changed to an unstable focus when the STC is suppressed by a periodic signal successfully. Such property change of the unstable fixed point allows the possibility of the oscillators with different time scales adjusting to perfect functional PS, in contrast to the imperfect one before the control. In the driving frame, two types of synchronization, frequency-locking, and multilooping PS are observed among the mode phases. For a few modes, frequency-locking occurs, whereas for other modes, multilooping PS occurs without frequency-locking. We find that if its frequency and intensity are properly chosen, an external periodic signal can cause the property change of a fixed point, which plays a crucial role in controlling STC to spatially regular state.

ACKNOWLEDGMENTS

This work is supported by the National Natural Science Foundation of China under Grants No. 10275007, No. 10335010, and No. 10475009.

[1] E. Ott, C. Grebogi, and J. A. Yorke, Phys. Rev. Lett. **64**, 1196 (1990).

[2] L. M. Pecora and T. L. Carroll, Phys. Rev. Lett. **64**, 821 (1990).

[3] W. L. Ditto, S. N. Rauseo, and M. L. Spano, Phys. Rev. Lett. **65**, 3211 (1990); E. R. Hunt, *ibid.* **67**, 1953 (1991).

[4] J. Singer, Y. Z. Wang, and H. H. Bau, Phys. Rev. Lett. **66**, 1123 (1991); A. Uchida, T. Sato, T. Ogawa, and F. Kannari, Phys. Rev. E **58**, 7249 (1998); A. N. Pisarchik and R. Corbalan, *ibid.* **59**, 1669 (1999); K. A. Mirus and J. C. Sprott, *ibid.* **59**, 5313 (1999).

[5] G. Hu and K. F. He, Phys. Rev. Lett. **71**, 3794 (1993); M. Markus, G. Kloss, and I. Kusch, Nature (London) **371**, 402 (1994); W. Lu, D. Yu, and R. G. Harrison, Phys. Rev. Lett. **76**, 3316 (1996); R. Montagne and P. Colet, Int. J. Bifurcation Chaos Appl. Sci. Eng. **8**, 1849 (1998).

[6] C. Tresser, P. A. Worfolk, and H. Bass, Chaos **5**, 693 (1995); L. Junge and U. Parlitz, Phys. Rev. E **62**, 438 (2000); R. Breban, *ibid.* **68**, 047201 (2003); B. Schelter, M. Winterhalder, R. Dahlhaus, J. Kurths, and Jens Timmer, Phys. Rev. Lett. **96**, 208103 (2006).

[7] N. F. Rulkov, M. M. Sushchik, L. S. Tsimring, and H. D. I. Abarbanel, Phys. Rev. E **51**, 980 (1995); H. D. I. Abarbanel, N. F. Rulkov, and M. M. Sushchik, *ibid.* **53**, 4528 (1996); L. Kocarev and U. Parlitz, Phys. Rev. Lett. **76**, 1816 (1996).

[8] M. G. Rosenblum, A. S. Pikovsky, and J. Kurths, Phys. Rev. Lett. **76**, 1804 (1996); E. Rosa, E. Ott, and M. H. Hess, *ibid.* **80**, 1642 (1998); R. Breban and E. Ott, Phys. Rev. E **65**, 056219 (2002).

[9] A. Neiman, X. Pei, D. Russell, W. Wojtenek, L. Wilkens, F. Moss, H. A. Braun, M. T. Huber, and K. Voigt, Phys. Rev. Lett. **82**, 660 (1999); N. H. Holstein-Rathlou, K. P. Yip, O. V. Sosnovtseva, and E. Moswkilde, Chaos **11**, 417 (2001); C. Schafer, M. G. Rosenblum, J. Kurth, and H. H. Abel, Nature (London) **392**, 239 (1998).

[10] I. Z. Kiss and J. L. Hudson, Phys. Rev. E **64**, 046215 (2001).

[11] M. A. Zaks, E.-H. Park, M. G. Rosenblum, and J. Kurths, Phys. Rev. Lett. **82**, 4228 (1999); E.-H. Park, M. A. Zaks, and J. Kurths, Phys. Rev. E **60**, 6627 (1999).

[12] S. G. Wu, K. F. He, and Z. Q. Huang, Phys. Lett. A **260**, 345 (1999).

[13] K. F. He and A. Salat, Plasma Phys. Controlled Fusion **31**, 123 (1989); R. K. Dodd, J. C. Eilbeck, J. D. Gibbon, and H. C. Morris, *Solitons and Nonlinear Wave Equations* (Academic Press, London, 1982), p. 596.

[14] K. F. He, Phys. Rev. Lett. **80**, 696 (1998).

[15] K. F. He, Int. J. Mod. Phys. B **18**, 1 (2004).

[16] K. He and Abraham C. L. Chian, Phys. Rev. Lett. **91**, 034102 (2003).

[17] N. F. Rulkov, M. M. Sushchik, L. S. Tsimring, and H. D. I. Abarbanel, Phys. Rev. E **51**, 980 (1995).